Yamanaka and Tanioka
Progress in Earth and Planetary Science (2022) 9:37
https://doi.org/10.1186/s40645-022-00496-1

Progress in Earth and Planetary Science

RESEARCH ARTICLE Open Access

Short-wave run-ups of the 1611 Keicho tsunami along the Sanriku Coast

Yusuke Yamanaka* and Yuichiro Tanioka

Abstract

A tsunami generated by an earthquake that occurred off the east coast of Japan in 1611 was predominantly concentrated along the Sanriku Coast. The 1611 event produced its greatest observed tsunami height at Koyadori, 28.8 m, higher than that produced by other representative tsunamis at the same location such as the 2011 Tohoku and 1896 Meiji Sanriku tsunamis. The characteristics of the source that resulted in the remarkable tsunami height at Koyadori have been widely debated. In this study, we simulated the local intensification mechanism of the 1611 tsunami and derived some key characteristics of the earthquake that produced the intensification at Koyadori based on these results. First, we investigated the topographical inundation characteristics in representative areas on the Sanriku Coast, including Koyadori, by numerical means. By comparing the numerical results with the observed heights for the 1611 tsunami, we found that a simulated tsunami that was dominated by short-wave components yielded a promising reproduction of the observed heights. The development of a local resonance seemed a more likely cause for the observed local intensification at Koyadori than a single-pulse wave. These results suggested that the 1611 earthquake produced a tsunami dominated by short-wave components. Furthermore, the source must have been located far off the Tohoku coast near the Japan Trench axis to have had substantial short-wave components along the Sanriku Coast. Based on these findings, we constructed a source scenario for local intensification by investigating the characteristics of Green's functions from single-point sources. The scenario involves two separate earthquake sources in shallow crustal areas at the plate interface of the subduction zone, resulting in a moment magnitude of 8.5. The tsunami produced by this source model, which reflected the characteristics of a tsunami earthquake, effectively reproduced the local intensification observed on the Sanriku Coast.

Keywords: Local intensification, Resonance, Green's function, Koyadori, Source characteristics, 1611 Keicho earthquake, Tsunami

1 Introduction

A tsunami generated by an earthquake in 1611 substantially damaged coastal areas on the Pacific Ocean side of the Tohoku region of Japan (hereafter, the 1611 Keicho tsunami and earthquake or 1611 tsunami and earthquake for short, respectively) (Fig. 1). This event is of such antiquity that eyewitness observations exist only in historical documents. Ebina and Imai (2014) have reviewed the historical documents, determined the observed tsunami heights along the coastline in the Tohoku region, and listed these heights alongside those provided by Hatori (1975), Tsuji et al. (2012, 2011), and Tsuji and Ueda (1995) to provide a review of the observed heights of the tsunami. As shown in Fig. 1, many of the observed tsunami heights were in the range of 0 to 10 m along the Tohoku coast, whereas the observed height was 28.8 m in a coastal area of Koyadori, which is located within the Sanriku Coast (Iwate Prefecture) in the Tohoku region (Figs. 1 and 2).

Koyadori is on a small peninsula between Yamada and Funakoshi Bays, in a small valley facing southeast. The valley at Koyadori terminates in a southeast-facing inlet

*Correspondence: yyamanaka@sci.hokudai.ac.jp

Institute of Seismology and Volcanology, Faculty of Science, Hokkaido University, Hokkaido, Japan

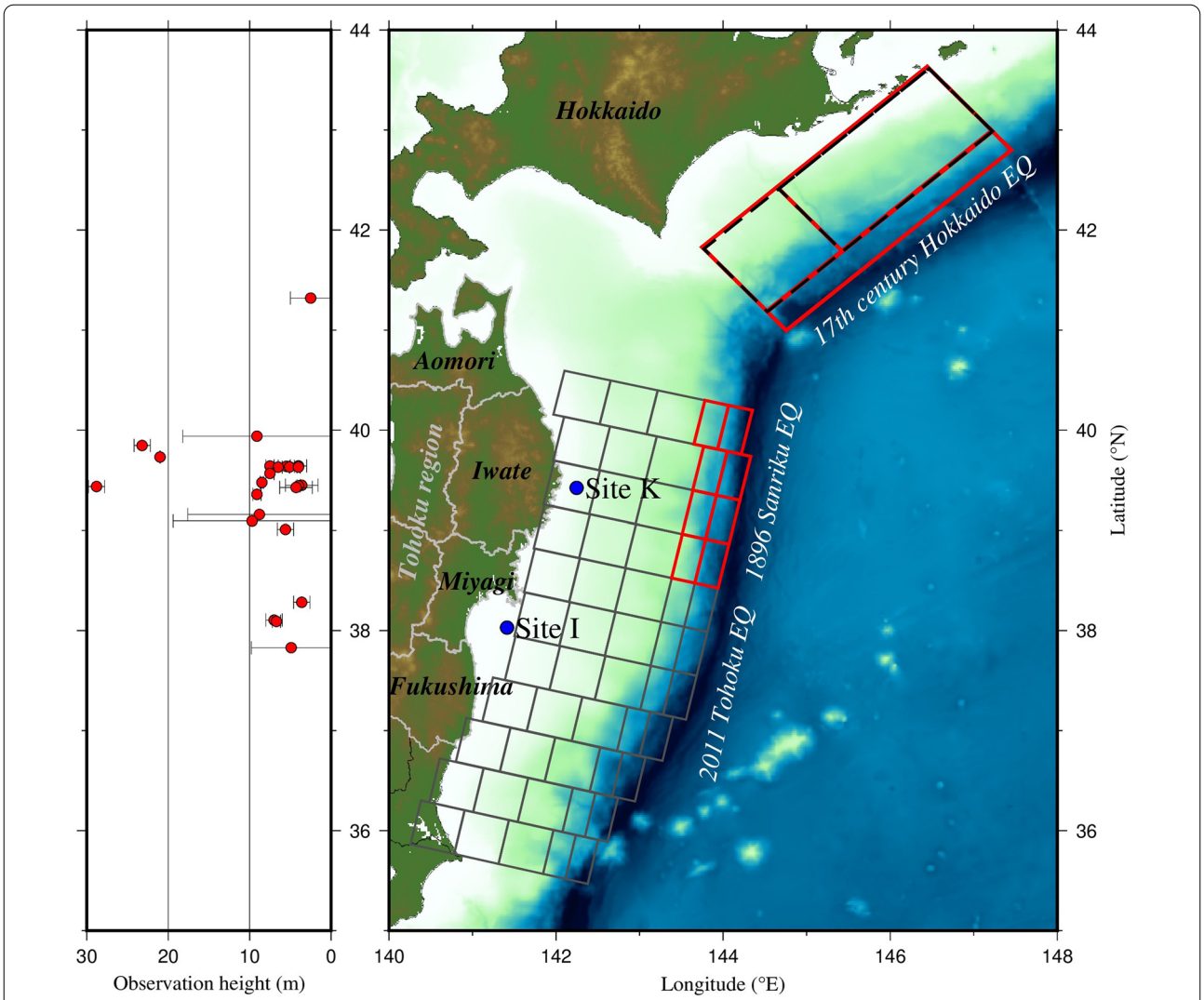

Fig. 1 Observed heights of the 1611 tsunami. The heights along the latitudinal direction reported by Ebina and Imai (2014) (including results from Hatori (1975), Tsuji et al. (2012, 2011), and Tsuji and Ueda (1995)) are displayed in the left panel, and representative source geometries in historical earthquakes indicated by squares are displayed in the right panel. The seventeenth-century earthquake source models were based on Ioki and Tanioka (2016) (red) and Okamura and Namegaya (2011) (black); the 1896 earthquake source model was based on Satake et al. (2017) (red); the 2011 earthquake source model was based on Satake et al. (2013) (gray)

at the edge of Funakoshi Bay. The tsunami height at Koyadori was derived from an event described in ancient folklore. According to this folklore, a tsunami, which could have been the 1611 tsunami, completely overflowed the valley from the inlet to reach the opposing Yamada Bay (e.g., Hatori 1975; Ishimura and Ebina 2021) (Fig. 2). Given this information, Ebina and Imai (2014) measured the altitude of the lowest pass between the two bays in the vicinity of Koyadori and determined that the tsunami height was 28.8 m. Existing studies have exhaustively investigated deposits left around Koyadori by historical tsunamis and have found those that may have been from the 1611 tsunami (Ishimura and Miyauchi 2015; Ishimura 2017). Ishimura and Ebina (2021) have reported that the above-mentioned folklore may predate the 1896 Meiji Sanriku tsunami; on the basis of their analysis of historical and geological evidence, they suggest that the overflow may have been generated by the 1611 tsunami. In this study, we have concluded, on the basis of the prior literature, that the 1611 tsunami completely overflowed the valley and that a height of 28.8 m may be a reliable observation, with small or moderate error. It is worthy of note that the 1896 Meiji Sanriku and 2011 Tohoku tsunamis, which seriously damaged the Tohoku coast,

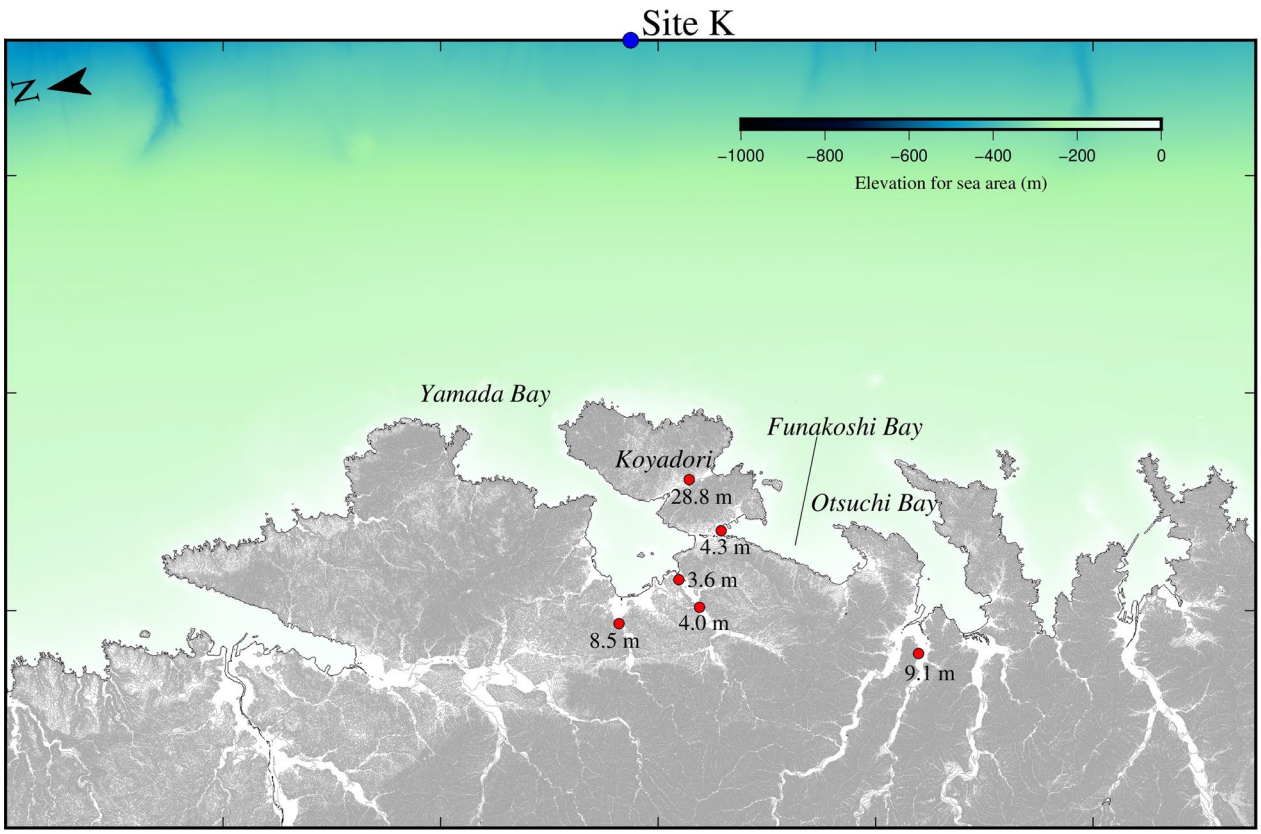

Fig. 2 Computational area considered for the numerical experiment. The upper boundary of the domain corresponds to an incident boundary, and red circles indicate targeted observation sites with the observed heights (Ebina and Imai 2014). The tick interval was 10 km

inundated the areas around Koyadori; however, neither of those tsunamis overflowed the valley completely (Ishimura and Ebina 2021). This observation suggests that the 1611 tsunami at Koyadori was more substantial than these two tsunamis.

The exact source of the 1611 tsunami (or the 1611 earthquake) remains unknown. In the 1900s, the source of the 1611 earthquake, with a magnitude of approximately 8.1, was thought to have been located off the Sanriku (Tohoku) Coast (e.g., Kawasumi 1951). Hatori (1975) proposed a source area for the 1611 earthquake roughly the same as that of the 1933 Showa Sanriku earthquake, with a normal fault type. According to Tsuji (1994), historical documents recorded substantial ground shaking but did not describe any resulting damage. Those observations suggest that the 1611 earthquake might have been a tsunami earthquake (e.g., Tsuji 1994; Watanabe 1997). In the 2000s, a different source area was proposed for the 1611 earthquake, based on a tsunami that was generated by an earthquake located along the Kuril Trench off the Hokkaido region in the seventeenth century (hereafter, the seventeenth-century Hokkaido tsunami and earthquake or the seventeenth-century tsunami and earthquake for short, respectively) (Fig. 1). The exact occurrence date and year for the seventeenth-century earthquake and tsunami remain unknown. Some studies speculate that the seventeenth-century tsunami might have seriously impacted the Tohoku coast as well as the Hokkaido coast (Okamura and Namegaya 2011; Hirakawa 2012). Those studies have proposed that the damage attributed to the 1611 tsunami along the Tohoku coast in previous studies may have in fact been from the seventeenth-century tsunami. Namely, that the seventeenth-century tsunami and the 1611 tsunami may have one and the same, generated off the coast of Hokkaido, and that no separate 1611 earthquake, having a source located off the Tohoku region, may have occurred. This scenario, in which a large earthquake (i.e., the seventeenth-century earthquake) occurred off the Hokkaido coast, far from the Tohoku coast, in 1611 can explain a situation where locals in the Tohoku region felt the ground to shake but did not observe significant damage (Tsuji 1994). According to historical documents, several ground shaking events occurred on the day of the 1611 earthquake in the Tohoku region, and the 1611 tsunami struck the Tohoku coast several hours after the large

ground shaking (e.g., Tsuji 1994; Tsuji and Ueda 1995). The time required for a locally generated tsunami to propagate from off the Tohoku coast would have been approximately 30 min; thus, a scenario in which the main source was located off the Hokkaido coast may be more credible than that in which the main source was located off the Tohoku coast (Okamura and Namegaya 2011). To elucidate the characteristics of tsunamis that impacted the Tohoku and Hokkaido coasts in the seventeenth century, Tetsuka et al. (2021) thoroughly reviewed existing studies and undertook the simulation of tsunamis from sources assigned to locations off the Hokkaido and Tohoku coasts.

As reviewed above, two dissimilar source areas have been proposed for the 1611 Keicho earthquake. In addition, recent studies have proposed different magnitudes from those in prior studies. Imai et al. (2015) developed a source model with a moment magnitude range of 8.4–8.7 and generated a tsunami that accorded with the observations reported by Ebina and Imai (2014). Fukuhara and Tanioka (2017) listed several coastal areas where the 1611 tsunami was larger than the 2011 tsunami and proposed a source scenario with a moment magnitude of 9.0 that was 250 km long and 100 km wide. That source model was developed by considering observations from large tsunamis, including the one at Koyadori. These reviews have demonstrated that the characteristics of the source area and the magnitude of the 1611 earthquake remain unknown and debated.

Figure 2 shows the tsunami heights observed around Koyadori for the 1611 tsunami. Moderate heights of up to 10 m were observed within several tens of kilometers from Koyadori, where a height of 28.8 m was observed. Despite the proximity of the observation sites, the 1611 tsunami had large variations in height. Accounting for this large variation will be key to any further understanding of both the 1611 tsunami and the 1611 earthquake. Fukuhara and Tanioka (2017) focused their attention on the tsunami height of 28.8 m, but they did not consider how the tsunami height variation was produced. In view of current gaps in knowledge, in this study, we have investigated the key factors responsible for the local intensification of the 1611 tsunami at Koyadori. We have also identified the source area and investigated the essential characteristics of the earthquake that generated such a local tsunami intensification.

2 Methods

2.1 Numerical experiments

Short-wave components in a tsunami are occasionally responsible for considerable local inundation and run-up heights. Shimozono et al. (2014) demonstrated that the short-wave components in the 2011 tsunami were responsible for the extreme run-up height observed in the Sanriku Coast. Yamanaka and Nakamura (2020) indicated that the substantially large run-up heights in a bay during the 1896 and 1933 tsunamis were characterized by short-wave components. By comparing the observations for the 1611 tsunami with simulation results obtained from a numerical experiment, we investigate the type of wave component most suitable for reproducing the large variation in tsunami height observed around Koyadori.

2.1.1 Inundation characteristics from parametric waves

For the numerical experiment, we introduced a parametric waveform as a product of sinusoidal and Gaussian functions (Shimozono et al. 2014; Yamanaka and Nakamura 2020):

$$\eta_0(t) = A_0 \cos\{\omega(t - t_0)\} \exp\left\{-\frac{\omega(t - t_0)^2}{2\alpha^2}\right\} \quad (1)$$

where η_0 denotes the water surface elevation change at the offshore boundary, A_0 denotes the wave amplitude, $\omega = 2\pi/T$ denotes the angular frequency with wave period T, t_0 denotes the time at which the peak of the primary wave appeared, and α (= 1, 2, or 3) is a nondimensional coefficient. Equation (1), with α values of 1, 2, and 3, introduces an up-pulse wave, a wave in which the initial decrease in water surface elevation occurs prior to the up-pulse, and a wave accompanied by a preceding wave, respectively (Fig. 3). These waves are comparable to N-waves (Tadepalli and Synolakis 1994). We determined the waveform as an incident boundary condition at the offshore (upper) boundary of the computational domain (Fig. 2), assigned a moving boundary condition at the boundary between the sea and land, and then simulated wave propagation and inundation by the primary wave in the domain based on a nonlinear long-wave model (Goto et al. 1997).

The resolution of the computational domain was 25 m, and the distribution of the elevation and still water depth in the domain was based on a digital elevation model sourced from the Geospatial Information Authority of Japan and the M7000 digital bathymetric chart provided by the Japan Hydrographic Association. It is important to note that we did not modify the constructed geometry; therefore, especially around shores, the present geometry may not necessarily correspond to that of 1611. The values for Manning's roughness were 0.030 and 0.025 $m^{-1/3}$ s for the land and water areas, respectively.

Yamada, Funakoshi, and Otsuchi Bays, and the inlet on Koyadori, for which differing heights of the 1611 tsunami were observed, are located close to each other (Fig. 2). Thus, the waves that impacted each of these four areas during the 1611 tsunami event can be

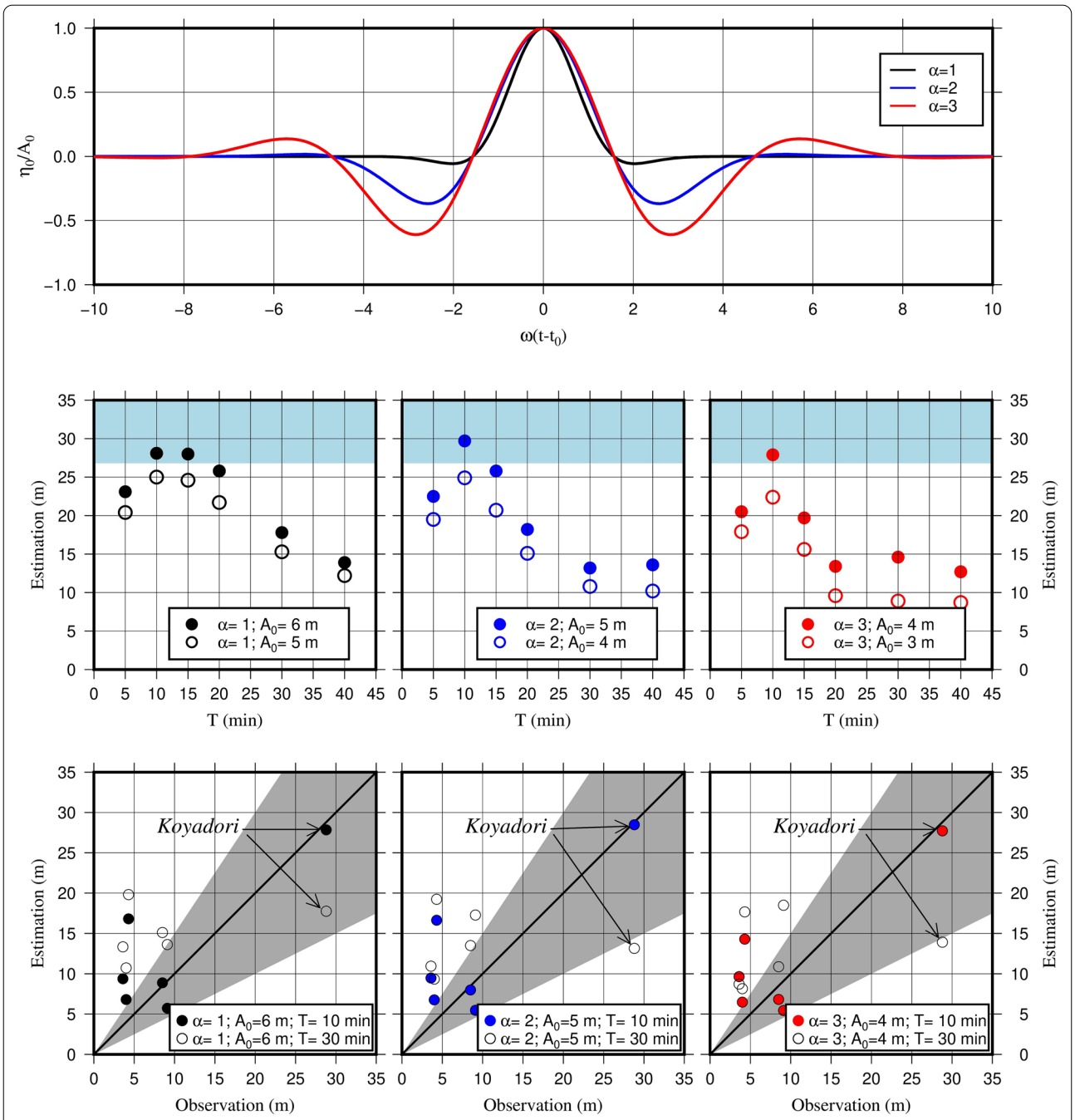

Fig. 3 Results of the numerical experiment. Incident waveforms (upper panel), maximum simulated height along the Koyadori valley (middle panels), and comparison of simulated heights and the observations (bottom panels). The gray area in the bottom panels indicates an error range within 50%

represented as similar or even identical to those that impacted the other three areas. We therefore compared the estimated inundation heights from the parametric wave with the observed heights of the 1611 tsunami to roughly determine the topographic inundation characteristics of these areas in 1611. When the observation site did not experience inundation in the simulation, the inundation height simulated near the site was compared with the observed height. Run-up heights in the observations were also compared with the simulated inundation heights. We did not consider changes in

water surface level due to astronomical tides in this study.

2.1.2 Propagation characteristics of historical tsunamis

To roughly determine the source location of the 1611 tsunami (i.e., the 1611 earthquake), we investigated historical tsunami propagation characteristics under four earthquake source scenarios: the seventeenth-century earthquake source models by Okamura and Namegaya (2011) and Ioki and Tanioka (2016); the 1896 earthquake source model by Satake et al. (2017); and the 2011 earthquake source model by Satake et al. (2013) (Fig. 1). Ioki and Tanioka (2016) successfully reproduced historical tsunami inundation on the Hokkaido coast, where deposits by the seventeenth-century tsunami were found. When comparing the source models constructed by Ioki and Tanioka (2016) with the source characteristics assumed by Okamura and Namegaya (2011) for the seventeenth-century earthquake, the former is characterized by a large shallow slip and might therefore produce more short-wave components at Koyadori than the latter.

We modeled the initial tsunami deformations as vertical displacements at the four sources, using the method of Okada (1985), and calculated the sea surface change after incorporating the effect of bathymetry (Tanioka and Satake 1996). The computational domain was obtained from the General Bathymetric Chart of the Oceans (GEBCO), which had a 30 arcsec resolution (Weatherall et al. 2015). We assigned a reflective boundary condition along the shores and then numerically solved the propagation of each deformation based on a linear long-wave model in a spherical coordinate system, which was derived from the model by Goto (1991) with a nondispersive assumption.

2.2 Analysis of Green's functions

We developed Green's functions for constraining the tsunami source area. Sea surface deformation, expressed as a two-dimensional Gaussian shape, was considered as an initial condition at $t=0$, in a similar manner to the work of Yamanaka et al. (2019).

$$\eta_G(x,y) = H \exp\left(-\frac{(x-x_0)^2-(y-y_0)^2}{2\sigma^2}\right) \quad (2)$$

where x and y denote rectangular coordinates and are functions of latitude and longitude, respectively; η_G denotes the initial water surface distribution; H denotes the height of the Gaussian shape at (x_0, y_0); and σ is a parameter representing the horizontal scale of the Gaussian shape. We determined that the horizontal scale was 5 km (Yamanaka et al. 2019) and assigned the Gaussian sources in a grid system by GEBCO, which has a spatial resolution of 30 arcsec (Weatherall et al. 2015), by changing the location of (x_0, y_0) with a five-grid interval in the latitudinal and longitudinal directions. We then simulated the propagation of each source (~6900 sources in total) based on a linear long-wave model (the model used in Sect. 2.1.2) and saved the waveforms simulated at the shores in Koyadori as Green's functions.

For Green's functions, the amplitude and time (as measured from the origin time) of the peak before the first zero-down crossing time are determined as η_p and t_p, respectively. We determined these parameters for Green's functions and expressed the phase of the primary wave propagating from the Gaussian source located at (x_0, y_0) to Koyadori for a wave period (T), as follows:

$$\varphi(x_0, y_0) = 2\pi \frac{t_p}{T} + C \quad (3)$$

where C is an arbitrary constant. By applying any wave period to T in Eq. (3), we obtained the phase characteristics of the primary waves for a specific wave period.

2.3 Source modeling

We tested an earthquake source scenario to estimate the 1611 tsunami (Table 1). The source geometries were modeled along with the subfault parameters shown in Satake et al. (2013). Source N, assigned to an area roughly the same as that of the 1896 earthquake, had a slip amount of 20 m; source S, assigned to another area, had a slip of 30 m. This source scenario reflects a moment magnitude of 8.5, assuming a rigidity of 2×10^{10} N/m^2, which is larger than the originally proposed magnitude of 8.1 (Kawasumi 1951; Hatori 1975) and smaller than the recent estimate of 9.0 (Fukuhara and Tanioka 2017).

We simulated tsunami propagation on the basis of the source scenario, using the linear long-wave model in a single spherical coordinate grid system to overview the

Table 1 Source scenario for the 1611 earthquake

Source	Length (km)	Width (km)	Depth (km)	Strike (°)	Dip (°)	Rake (°)	Slip (m)	Lat. (°)	Lon. (°)
N	100	75	0	193	8	81	20	39.738	144.331
S	75	75	0	193	8	81	30	37.986	143.810

The definition of each parameter is the same as that by Satake et al. (2013)

large-scale impacts of the tsunami. In addition, we simulated the tsunami inundation for an area around Koyadori using linear and nonlinear long-wave models in spherical coordinate grids with a two-way nested grid system (Imamura et al. 2006). The computational conditions are listed in Additional file 1: Table S1 We combined four computational geometries with spatial resolutions of 30, 10, 10/3, and 10/9 arcsec in a nested grid system. The computational conditions for the propagation simulation corresponded to those for the inundation simulation in Geometry 1 (Additional file 1: Table S1). As in Sect. 2.1.1, for the finest computational domain of the nested grid system (Geometry 4), no historical modification of the constructed geometry was undertaken, and the Manning's roughness values were input as 0.030 and 0.025 $m^{-1/3}$ s for the land and water areas, respectively; we also, once more, assigned a moving boundary condition at the boundary between the sea and land and did not consider changes in the tide level in the computation. To demonstrate the impact of each source in the model, we simulated tsunami inundation for an hour after the earthquake under three scenarios using sources N, S, and N and S.

3 Results and discussion

3.1 Numerical experiments

The upper panel in Fig. 3 shows the incident parametric waveforms for different values of α, and the middle panels display the maximum simulated heights of the waves at the wavefront along the Koyadori valley. In the middle panels, the markers plotted within the blue area indicate that the wave completely overflowed the valley to reach Yamada Bay. According to the results of our simulation, waves with a short period (approximately 10 min) overflowed the Koyadori valley. The bottom panels in Fig. 3 compare the observations and the results simulated using parametric incident waves at the corresponding locations. An incident wave with a shorter wave period could more accurately reproduce the large variation than that with a longer wave period. On the basis of these results, we concluded that a short-wave-dominated tsunami struck Koyadori in 1611.

As shown in Fig. 3, the magnitude of the incident wave amplitude required for overflow decreased as α increased. The middle-right panel in Fig. 3 shows that waves with a wave period of approximately 10 min effectively produced the largest inundation height along the Koyadori valley. This is because the waves enhanced the local resonance at the inlet of Koyadori (Fig. 2). To identify the resonance period of the inlet, we conducted an additional numerical experiment using a parametric waveform with $\alpha = 3$. For the computation, we used a linearized long-wave model to estimate pure resonance characteristics in sea areas. Additional file 1: Fig S1 compares the values of the maximum increase in water surface elevation due to the wave (η_{max}) normalized by the incident wave amplitude (A_0) at the head of the inlet for each wave period (T). This figure shows that the maximum water surface elevation peaked at approximately 7–8 min. On the basis of this result, we determined that the resonance period of the inlet (T_r) was 8 min.

Figure 4 shows the time series of change in the water surface elevation from the mean sea level (η) simulated at sites K and I indicated in Figs. 1 and 2 under the historical earthquake source scenarios and with the introduction of a parameterized waveform based on Eq. (1), with values of t_0, A_0, and T to fit the simulated waveform. By comparing the parameterized and simulated waveforms at site K, we found that the tsunamis under the source scenarios described by Okamura and Namegaya (2011) and Ioki and Tanioka (2016) had a substantial wave component at approximately 30 min, which is inconsistent with the wave characteristics expected for Koyadori during the 1611 tsunami. The 2011 tsunami had both short- and long-wave components with periods of approximately 10 and approximately 30 min, respectively. The 1896 tsunami was also well represented by a parameterized waveform assuming a wave period of 6 min. This type of short-wave component, generated by large slips in shallow areas along the plate interface of the subduction zone, can be considered to produce the local intensification observed at Koyadori in 1611. On the basis of these results, we concluded that the source of the 1611 tsunami (i.e., the 1611 earthquake) was located off the Tohoku coast, rather than off the Hokkaido coast. Given the short-wave components required to produce local tsunami intensification and the insignificant damage caused by the earthquake, the 1611 earthquake might have been a tsunami earthquake, as previously reported (Tsuji 1994; Watanabe 1997).

The 1611 earthquake characteristics should have been more like those of the 1896 earthquake than of the 2011 earthquake, if the 1611 earthquake was a tsunami earthquake. However, as shown in Fig. 4, the 1896 tsunami was muted at site I, located off Miyagi Prefecture. Existing studies have also reported that a large tsunami inundation occurred along the coastline of Miyagi Prefecture. Iwanuma City, located in the prefecture (around 38.1 °N and 140.9 °E), experienced considerable inundation during the 1611 tsunami (e.g., Tsuji and Ueda 1995). An earthquake with the same source area as the 1896 earthquake and larger slips than those determined by Satake et al. (2017) might reproduce the tsunami observed around Koyadori in 1611, but it is unlikely that it would have produced a large inundation along the Miyagi coast. It is therefore necessary to generate a slip distribution for

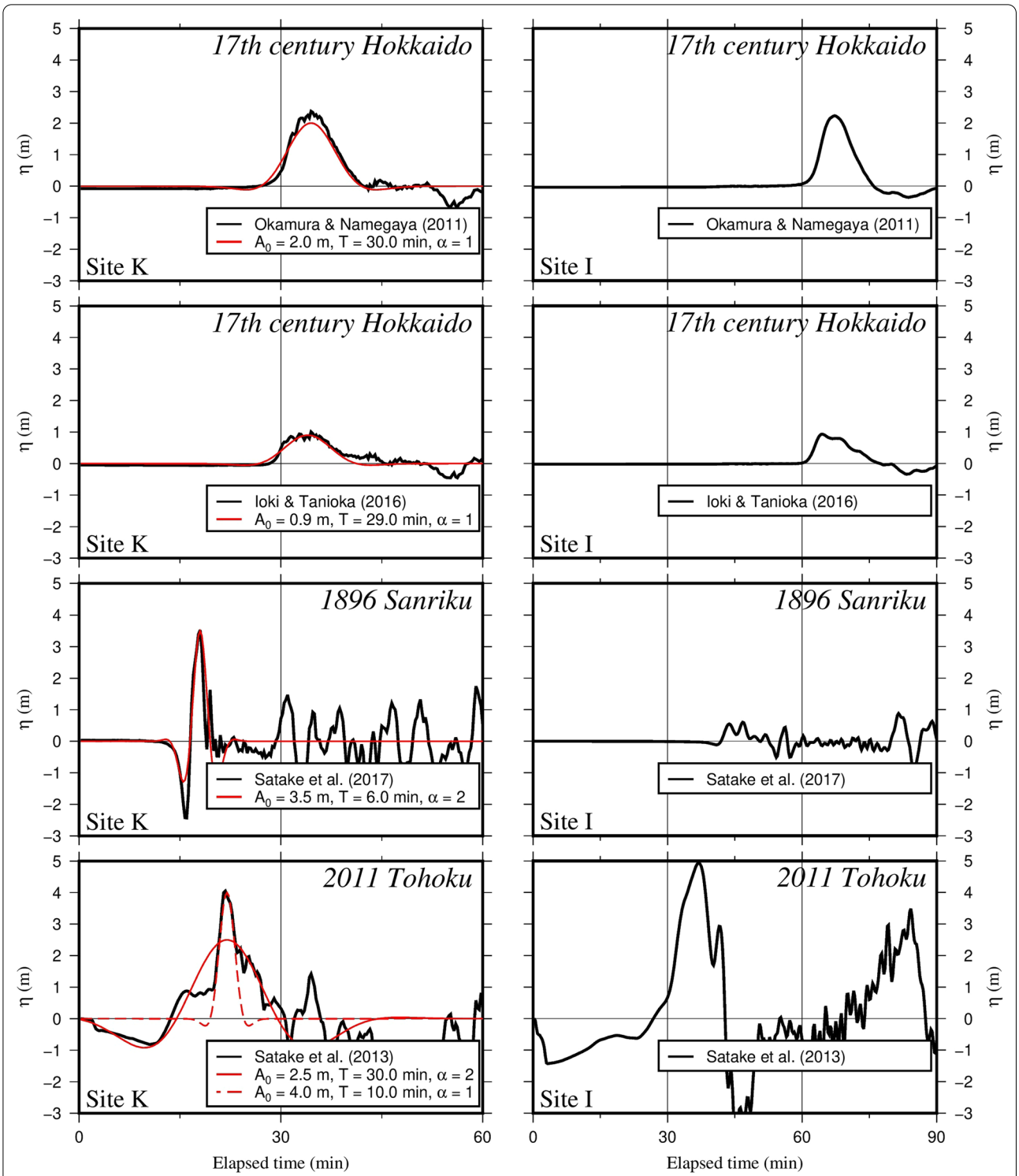

Fig. 4 Simulated waveforms at site K (left) and site I (right). These are the waveforms under the four earthquake source scenarios indicated in Fig. 1. Red lines are the waveforms that we parameterized using Eq. (1) for the simulated waveforms

the 1611 earthquake that can produce both the short-wave components of the tsunami around Koyadori and a tsunami considerably impacting the Miyagi coast.

3.2 Analysis of Green's functions

Figure 5a shows the distribution of η_p (x_0, y_0) normalized by the Gaussian height (H) and therefore indicates the sensitivity of the source locations to the peak amplitude at Koyadori. The source geometries determined by Fujii et al. (2011) and Satake et al. (2013) for the 2011 earthquake are also shown in the same figure. Satake et al. (2017) used these geometries to develop a source model of the 1896 earthquake. As shown in Fig. 5a, the primary waves from sources located near Koyadori had a strong impact; the impact decreased as the source location moved away from Koyadori. However, comparing the impacts from the sources located closer to Miyagi (around F3–F4 and G3–G4) and areas further offshore (around F0–F2 and G0–G2), the Gaussian sources located around F0–F2 and G0–G2 had a large impact on Koyadori. Figure 5b shows the distribution of cosine ϕ (x_0, y_0) with $T = T_r$ (8 min) to present continuous phase changes in space and, therefore, an overview of the relative phase characteristics of the primary waves with a wave period of 8 min. We have assumed that the 1611 earthquake was a tsunami earthquake and that the 1611 tsunami produced a bay-scale (inlet-scale) resonance that substantially impacted Koyadori. This phase distribution map is then useful for determining the location of sources, enabling the production of local bay-scale resonance. The source areas for the Gaussian distribution are alternately colored red and green in the figure, along the direction of the primary wave propagation. The gaps between the red or green bands, respectively, correspond to a wave period of approximately 8 min. When two sources were, respectively, contained in different red (or green) band areas across a green (or red) band area, as shown in Fig. 5b, the primary wave from the sources would arrive at Koyadori with a time difference of approximately 8 min.

We assumed that the 1611 earthquake produced a substantial slip in nearly the same area as that of the 1896 earthquake (Satake et al. 2017) and, therefore, determined the corresponding source areas to be in the vicinity of the grid rectangles B0, B1, C0, and C1 in Fig. 5. If the 1611 tsunami was generated by a tsunami earthquake, slips would have concentrated in the shallower areas of the subduction zone. Thus, substantial slips should have occurred within the areas of columns 0, 1, and 2 (Fig. 5). Consequently, to produce a tsunami generating bay-scale resonance in combination of primary waves, another source should be located around the source grid rectangles F0, F1, and F2. The areas around F0, F1, and F2 correspond moderately

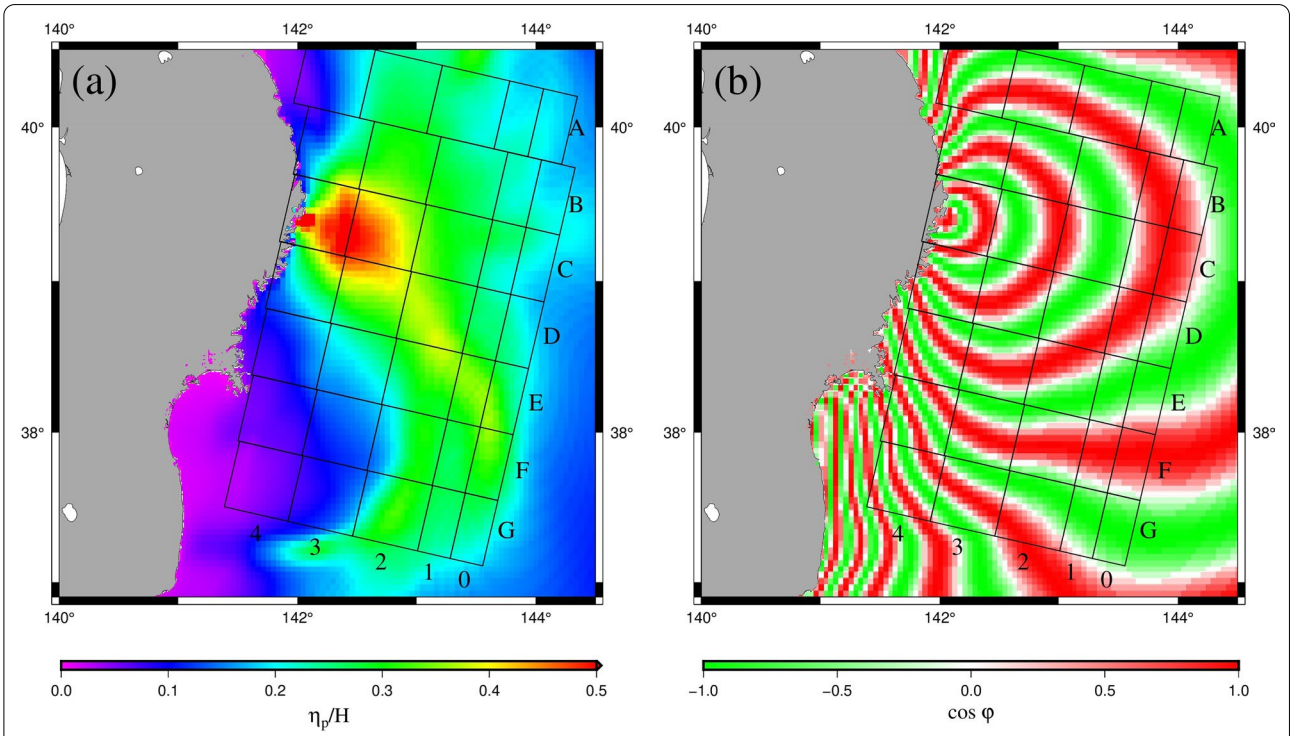

Fig. 5 Distributions of the maximum amplitude in the primary wave (η_p) and phase (φ) for a wave period of 8 min (**a** and **b**)

to the areas where the 2011 earthquake fault ruptured most greatly (Fujii et al. 2011; Satake et al. 2013). The two source areas assumed in Table 1 have covered the source areas of the rectangles B0, B1, C0, and C1 and the rectangles F0, F1, and F2, respectively.

3.3 Source modeling

Based on the tsunami propagation simulation, Fig. 6 shows the initial tsunami deformation estimated using the methods of Okada (1985) and Tanioka and Satake (1996), and a snapshot of its propagation. As shown in the figure, the initial deformation completely separated into two areas (Fig. 6a), and the primary waves from the two deformations arrived at Koyadori with a time difference (Fig. 6b). Small displacements between the two source areas are essential to generate resonance at Koyadori. Because we assigned source S off Miyagi Prefecture with a large slip, in addition to the generation of local resonance impacting Koyadori, a large inundation could also be expected along the coastline of Miyagi (Additional file 1: Fig S2), as reported in previous studies (e.g., Tsuji 1994; Tsuji and Ueda 1995).

On the basis of the tsunami inundation simulation, Fig. 7 shows snapshots of the water surface elevation change from the mean sea level (η) near Koyadori for the three scenarios at the corresponding time. For the scenario with source N, the primary wave impacted Koyadori 25 min after the earthquake, and free oscillation appeared within the inlet 35 min after the earthquake. However, the tsunami did not overflow the Koyadori valley completely. For the scenario with source S, the primary wave required a longer time (approximately 35 min after the earthquake) to impact Koyadori, again without overflowing the valley. This arrival time is consistent with a time at which the water surface level increased because of the free oscillation for the scenario with source N. In the scenario with sources N and S, the primary wave from source S is superposed on the free oscillation excited by the primary wave from source N, observed 35 min after the earthquake. Resonant oscillation was therefore enhanced at approximately 35 min; as a result, the tsunami flooded over the rim of the valley to reach Yamada Bay, as indicated in the bottom-center and right panels in Fig. 7.

Figure 8 displays a simulated inundation area based on the scenario with sources N and S and compares the simulated and observed tsunami heights. As shown in Fig. 8a, a moderate height of 4.3 m was observed approximately 3 km west of Koyadori. The tsunami was overestimated at this site under the current scenario with sources N and S. However, we successfully reproduced the considerable variation between the heights, as indicated in

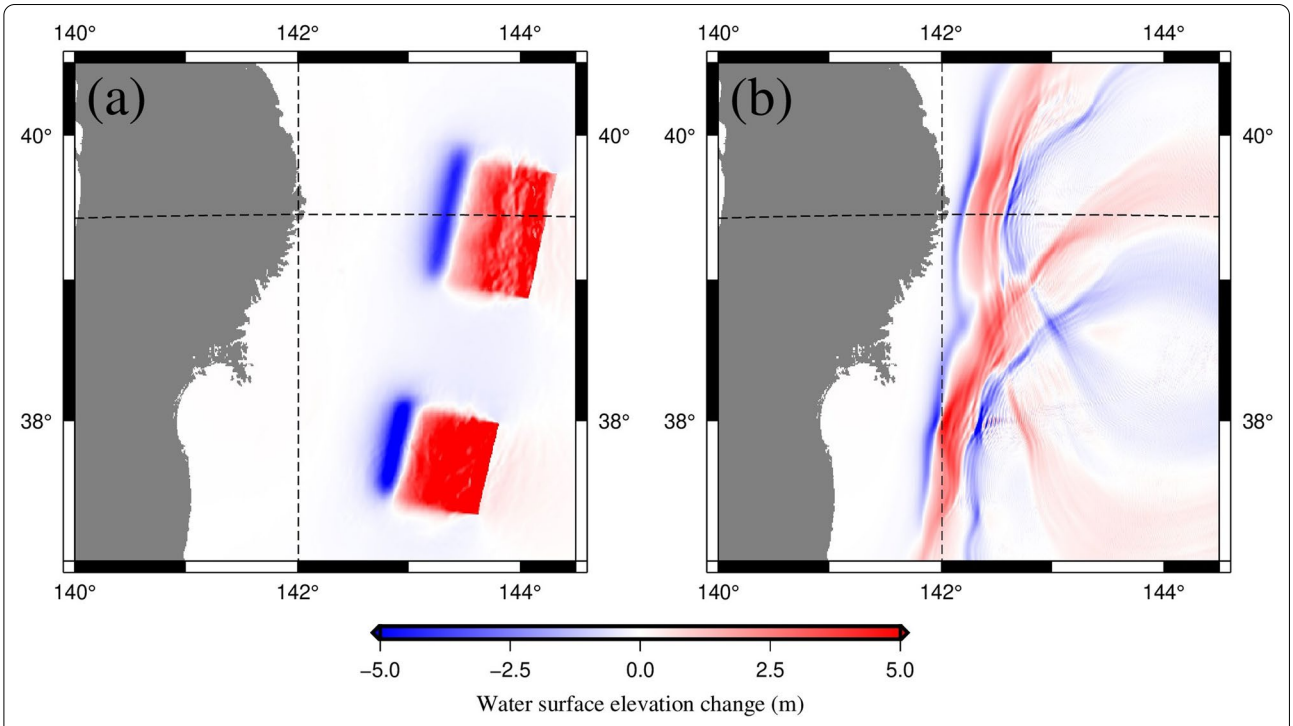

Fig. 6 Snapshots of (**a**) the initial tsunami deformation and (**b**) tsunami propagation. The point at which the two dashed lines cross indicates the location of Koyadori

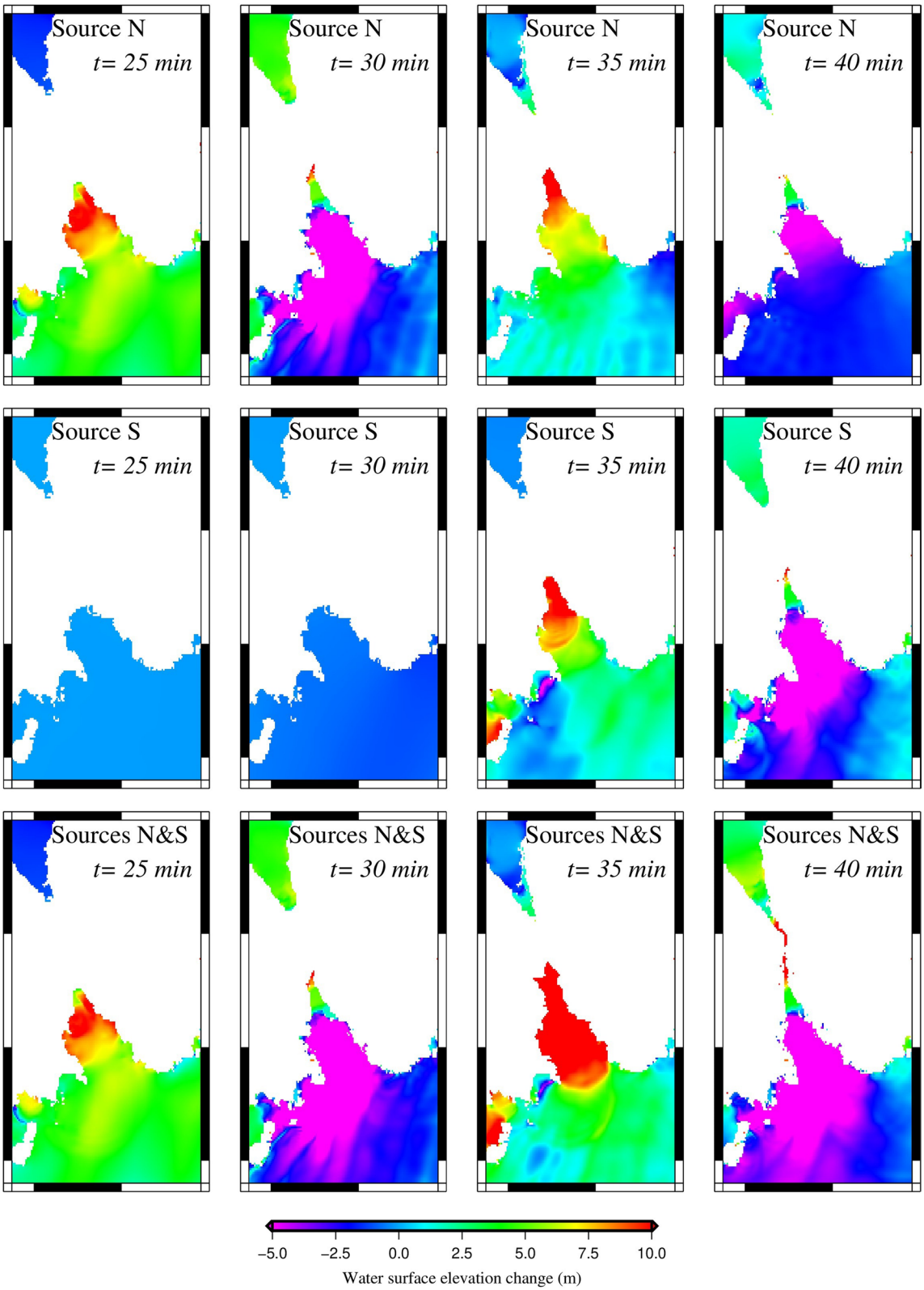

Fig. 7 Snapshots of tsunami propagation and inundation around the valley of Koyadori. The upper, middle, and bottom panels provide the results for the scenarios with sources N, S, and N and S, respectively

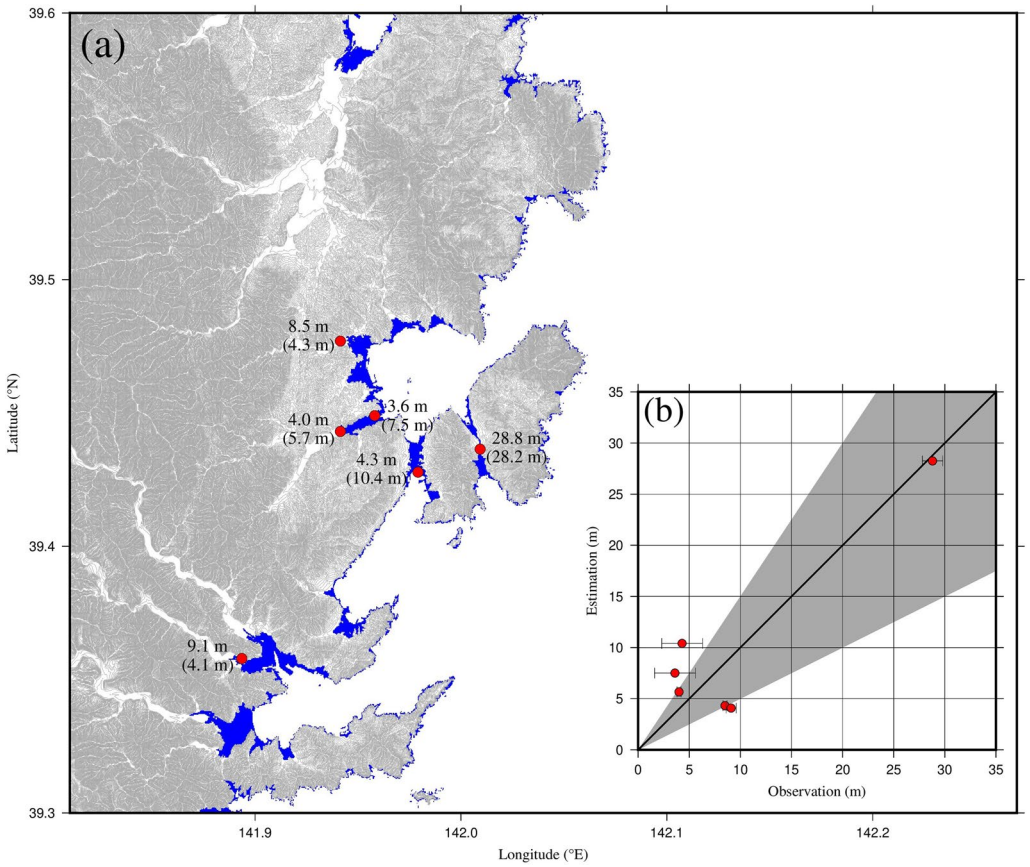

Fig. 8 Simulated inundation area (blue) under the scenario with sources N and S, and a comparison of the simulated heights and observations. The simulated heights are displayed to follow the observed values from the observation sites (red circle) in (**a**). The magnitude of the error in (**b**) is the one shown in Ebina and Imai (2014), and the gray area indicates an error range within 50%

the figure, and reproduced the other observed heights with moderate accuracy (Fig. 8b). Considering the results shown in Figs. 7 and 8, the two separated sources along the plate interface can at least reproduce the variation in tsunami heights observed in the bays and, by resonance, the maximum tsunami height observed at Koyadori. Therefore, the tested scenario might be considered one that reasonably reflects the essential characteristics of the 1611 earthquake. We note that the slips assumed for the two source areas have a complementary relationship in the production of a locally concentrated tsunami at Koyadori. For example, local intensification can also be produced in a scenario that involves larger and smaller slips than those shown in Table 1 in one and the other of the areas.

4 Conclusions

We investigated the local intensification characteristics of the 1611 Keicho tsunami using numerical simulation. The findings of the numerical experiment indicated that the observed tsunami heights at Koyadori and Otsuchi, Funakoshi, and Yamada Bays were predominantly characterized by short-wave components. Existing studies have reported contradictory results with respect to the source of the 1611 Keicho earthquake and tsunami and have proposed possible source areas off the Tohoku and Hokkaido coasts, respectively. According to our simulation results, tsunamis generated by source models (Okamura and Namegaya 2011; Ioki and Tanioka 2016) assigned to a region off the Hokkaido coast did not have large wave components at shorter wave periods near Koyadori. By contrast, a tsunami generated off the Tohoku region was able to manifest short-wave components if a large slip occurred in an earthquake in the shallow areas of the subduction zone. These results indicated that the source of the 1611 tsunami was located off the Tohoku coast and that the 1611 earthquake might have been a tsunami earthquake. Our simulation results also showed that multiple waves generating local resonance, rather than a single large wave, could be the main factor responsible for the observed inundation characteristics. By investigating the phase

characteristics with the aid of Green's functions, we proposed a possible earthquake source scenario for producing local resonance. The moment magnitude of the earthquake in the model was 8.5, and the tsunami produced by the source reasonably reproduced the observed inundation characteristics around Koyadori. The observed height at Koyadori for the 1611 tsunami was larger than that of the 2011 tsunami. However, these observation results do not necessarily indicate that the 1611 earthquake produced larger spatial sea surface deformation than that produced by the 2011 earthquake. This is because our findings demonstrated that two substantial tsunami deformations, each generated in a local confined area, could have produced wavetrains that combined to excite resonance and cause the substantial inundation of Koyadori.

Because it occurred in a less scientific era than today, quantitative observational data, such as tide gauge records, do not exist for the 1611 tsunami. However, in this study, we successfully identified the wave characteristics of the 1611 tsunami (i.e., a dominant wave period) by thoroughly comparing the simulated results with the observed tsunami heights. Consequently, we specified the tsunami source area as being in the Tohoku region and successfully constructed a source scenario that might reflect the essential characteristics of the earthquake. Therefore, investigating and specifying the wave components of tsunamis generated during other historical earthquakes may be important for the development of accurate earthquake source models. Our source scenario for the 1611 earthquake strongly relied on the tsunami characteristics observed around Koyadori, includes uncertainties, and thus requires further verification. The tsunami characteristics observed along other coasts must also be investigated to develop a more accurate source model.

Abbreviation

GEBCO: General Bathymetric Chart of the Oceans.

Supplementary Information

The online version contains supplementary material available at https://doi.org/10.1186/s40645-022-00496-1.

Additional file1: **Table S1**. Computational conditions. **Fig. S1**. Relationship between the wave period and the normalized maximum water surface elevation observed at the inlet head. **Fig. S2**. Comparison of observed and simulated heights for the 1611 tsunami and geometries of the sources assumed in this study.

Acknowledgements

We thank our scientific editor (Prof. Ryota Hino) and two anonymous reviewers for their constructive comments on improving the manuscript. The figures presented in this paper were created using the Generic Mapping Tools (GMT) software of Wessel et al. (2013).

Author contributions

YY conducted the numerical simulation and analyzed the simulation results with YT; both authors read and approved the final manuscript.

Funding

This study was supported by the Ministry of Education, Culture, Sports, Science and Technology (MEXT) of Japan, under The Second Earthquake and Volcano Hazards Observation and Research Program (Earthquake and Volcano Hazard Reduction Research).

Availability of data and material

The data presented are available from the corresponding author on request.

Declarations

Competing interests

The authors declare that they have no competing interests.

Received: 3 February 2022 Accepted: 18 June 2022
Published online: 06 July 2022

References

Ebina Y, Imai K (2014) Tsunami traces survey of the 1611 Keicho Ohsyu earthquake tsunami based on historical documents and traditions. Research Report Tsunami Eng 31:139–148 (**In Japanese**)

Fujii Y, Satake K, Sakai S, Shinohara M, Kanazawa T (2011) Tsunami source of the 2011 off the Pacific coast of Tohoku earthquake. Earth Planets Space 63:815–820. https://doi.org/10.5047/eps.2011.06.010

Fukuhara G, Tanioka Y (2017) Fault model of the 1611 Keicho tsunami earthquake (Mw9.0) estimated from historical documents using tsunami inundation simulation. Abstract in JpGU-AGU Joint Meeting 2017, HDS16–10.

Goto C, Ogawa Y, Shuto N, Imamura F (1997) Numerical method of tsunami simulation with the leap-frog scheme (IUGG/IOC Time Project). IOC Manual. United Nations Educational, Scientific and Cultural Organization, 35.

Goto C (1991) Numerical Simulation of the Trans-oceanic Propagation of Tsunami. rep, 30. Port and Harbour Research Institute, pp 4–19. (**In Japanese**).

Hatori T (1975) Tsunami magnitude and wave source regions of historical tsunamis in northeast Japan. Bull Earthquake Res Inst Univ Tokyo 50:397–414 (**In Japanese with English abstract**)

Hirakawa K (2012) Outsize tsunami sediments since last 6000 year as along the Japan- and Kuril-Trench: a tentative idea and sources and supercycle. Kagaku 82:172–181 (**In Japanese**)

Imai K, Maeda T, Iinuma T, Ebina Y, Sugawara D, Imamura F, Hirakawa A (2015) Paleo tsunami source estimation by using combination optimization algorithm: case study of the 1611 Keicho earthquake. Tohoku J Nat Disaster Sci 51:139–144 (**In Japanese**)

Imamura F, Yalciner AC, Ozyurt G (2006) Tsunami modeling manual. https://www.tsunami.irides.tohoku.ac.jp/media/files/_u/project/manualver-3_1.pdf.

Ioki K, Tanioka Y (2016) Re-estimated fault model of the 17th century great earthquake off Hokkaido using tsunami deposit data. Earth Planet Sci Lett 433:133–138. https://doi.org/10.1016/j.epsl.2015.10.009

Ishimura D (2017) Re-examination of the age of historical and paleo-tsunami deposits at Koyadori on the Sanriku Coast, northeast Japan. Geosci Lett 4:1–12. https://doi.org/10.1186/s40562-017-0077-4

Ishimura D, Ebina Y (2021) Historical and geological examination of the tradition at the watershed between Koyadori and Oura, Yamada town, Iwate prefecture. Historical Earthquakes 36:89–97 (**In Japanese with English abstract**)

Ishimura D, Miyauchi T (2015) Historical and paleo-tsunami deposits during the last 4000 years and their correlations with historical tsunami events in Koyadori on the Sanriku Coast, northeastern Japan. Prog Earth Planet Sci 2:16. https://doi.org/10.1186/s40645-015-0047-4

Kawasumi H (1951) Measures of earthquake danger and expectancy of maximum intensity throughout Japan as inferred from the seismic activity in historical times. Earthquake Research Inst Univ Tokyo 29:469–482

Okada Y (1985) Surface deformation due to shear and tensile faults in A half-space. Bull Seismol Soc Am 75:1135–1154. https://doi.org/10.1785/BSSA0750041135

Okamura Y, Namegaya Y (2011) Reconsideration of the 17th century Kuril multi-segment earthquake. Annu Rep Act Fault Paleoearthquake Res 11:15–20 (**In Japanese with English abstract**)

Satake K, Fujii Y, Harada T, Namegaya Y (2013) Time and space distribution of coseismic slip of the 2011 Tohoku earthquake as inferred from tsunami waveform data. Bull Seismol Soc Am 103:1473–1492. https://doi.org/10.1785/0120120122

Satake K, Fujii Y, Yamaki S (2017) Different depths of near-trench slips of the 1896 Sanriku and 2011 Tohoku earthquakes. Geosci Lett 4:33. https://doi.org/10.1186/s40562-017-0099-y

Shimozono T, Cui H, Pietrzak JD, Fritz HM, Okayasu A, Hooper AJ (2014) Short wave amplification and extreme runup by the 2011 Tohoku tsunami. Pure Appl Geophys 171:3217–3228. https://doi.org/10.1007/s00024-014-0803-1

Tadepalli S, Synolakis CE (1994) The run-up of N-waves on sloping beach. Proc R Soc Lond A 445:99–112. https://doi.org/10.1098/rspa.1994.0050

Tanioka Y, Satake K (1996) Tsunami generation by horizontal displacement of ocean bottom. Geophys Res Lett 23:861–864. https://doi.org/10.1029/96GL00736

Tetsuka H, Goto K, Ebina Y, Sugawara D, Ishizawa T (2021) Historical and geological evidence for the seventeenth-century tsunamis along Kuril and Japan trenches: implications for the origin of the AD 1611 Keicho earthquake and tsunami, and for the probable future risk potential. Geol Soc London Spec Publ 501:269–288. https://doi.org/10.1144/SP501-2019-60

Tsuji Y, Ueda K (1995) Investigation of the 1611, 1677, 1763, 1793, and 1856 tsunamis generated by earthquakes in the Sanriku region. Hist Earthquakes 11:75–106. (**In Japanese; Translated title**)

Tsuji Y, Mabuchi Y, Oie T, Imamura F (2011) Field survey for the 1611 tsunami along coasts of Iwate Prefecture. Res Rep Tsunami Eng 28:173–180

Tsuji Y, Imai K, Mabuchi Y, Oie T, Okada K, Iwabuchi Y, Imamura F (2012) Field survey of the tsunami of the 1677 Empo Boso-oki and the 1611 Keicho Sanriku-oki earthquake. Res Rep Tsunami Eng 29:189–207. (**In Japanese**)

Tsuji Y (1994) Historical tsunami earthquakes. Chikyu MON 16:73–85. (**In Japanese; Translated title**).

Watanabe H (1997) A study on the 1611 Keicho Sanriku tsunami and earthquake. Res Rep Tsunami Eng 14:79–88

Weatherall P, Marks KM, Jakobsson M, Schmitt T, Tani S, Arndt JE, Rovere M, Chayes D, Ferrini V, Wigley R (2015) A new digital bathymetric model of the world's oceans. Earth Space Sci 2:331–345. https://doi.org/10.1002/2015EA000107

Wessel P, Smith WHF, Scharroo R, Luis JF, Wobbe F (2013) Generic mapping tools: improved version released. Eos, Trans Am Geophys Union 94:409–410. https://doi.org/10.1002/2013EO450001

Yamanaka Y, Nakamura M (2020) Frequency-dependent amplification of the Sanriku tsunamis in Ryori Bay. Earth Planets Space 72:1–14. https://doi.org/10.1186/s40623-019-1128-1

Yamanaka Y, Sato S, Shimozono T, Tajima Y (2019) A numerical study on nearshore behavior of Japan Sea tsunamis using Green's functions for Gaussian sources based on the linear Boussinesq theory. Coast Eng J 61:187–198. https://doi.org/10.1080/21664250.2019.1579462

Publisher's Note